

Cramér-Rao Lower Bound on Time of Arrival Estimates for an Envelope-Detected Pulse

Anne M. Zelnio*, Linda J. Moore*, Craig R. Roush[‡], and Brian D. Rigling[†]

*Sensors Directorate

Air Force Research Laboratory, WPAFB, OH 45433

[‡]n-ask

Aurora, Colorado 80016

[†]Department of Electrical Engineering

Wright State University, Dayton, OH 45435

Abstract—The pulse time of arrival is an important parameter estimated in an electronic warfare receiver. The Cramér-Rao bound provides a lower bound on the variance of unbiased parameter estimates. In the past, time of arrival performance has been compared to a bound derived under Gaussian assumptions. However, these estimates are frequently computed from the pulse envelope, which exhibits Rician statistics that are approximately Gaussian only at high signal-to-noise ratios. This correspondence derives the Rician Cramér-Rao bound on time of arrival estimation accuracy.

I. INTRODUCTION

In electronic warfare (EW), receivers are designed to observe adversary waveforms and estimate their key parameters for purposes of system classification and threat identification. As the sheer size of the library of candidate waveforms rules out coherent processing, pulse parameters are frequently determined from the signal envelope. Pulse envelope processing allows the receiver to be effective against a large class of radar signals without a priori information about the adversary's phase modulation. Providing the highest accuracy possible in parameter estimates maximizes classification and identification performance [1]. In the design process, engineers must determine the accuracy with which they can measure pulse parameters at different power levels. Such systems engineering analysis is then fed back into larger system models to determine the effectiveness of the EW receiver in certain scenarios. Some exemplar EW receiver architectures are well-documented in [2]–[4].

In pulse envelope processing, an EW system typically estimates time of arrival (TOA), amplitude, and pulse width. Further exploitation of these estimates must incorporate knowledge of parameter estimate accuracy. Algorithm performance can be measured empirically through Monte Carlo simulations. However, it is important to compare these measurements to a tight theoretical bound on estimation accuracy. The Cramér-Rao Lower Bound (CRLB) [5], which provides a lower bound on the variance of unbiased parameter estimates, is a tool for analyzing algorithm performance.

Previous work [6] has presented the CRLB derivation for frequency, amplitude, time of arrival, and phase for a single pulse under Gaussian assumptions. However, while fairly

effective at high SNR, this approach does not provide a tight bound when applied to the envelope detector. As shown in Section II, the output of the envelope detection operation is a Rician distributed random process that appears Gaussian only at high SNR (e.g., $\geq 20\text{dB}$).

This paper derives the CRLB on parameter estimates from an envelope detected pulse, with emphasis on time of arrival. Section II introduces the pulse envelope signal model. Section III presents the derivation of the CRLB under Rician statistics. Section IV gives simulation results. Finally, Section V concludes with a summary of results and future work.

II. RECEIVED SIGNAL MODEL

The signal digitized by the EW receiver with discrete-time index n with sampling interval T_s ,

$$x_n = a_n \exp\{j\phi_n\} + w_n, \quad n = 1 \dots N \quad (1)$$

is assumed to consist of a band-limited rectangular pulse a_n with an unknown phase function ϕ_n corrupted by white Gaussian noise w_n with variance σ^2 . The pulse envelope a_n is defined by parameters that determine its amplitude, rise and fall behavior. The signal x_n is thus Gaussian distributed with mean $\mu_n = a_n \exp\{j\phi_n\}$ and covariance $k_{n_1, n_2} = \sigma^2 \delta_{n_1 - n_2}$. CRLB analysis of such a Gaussian signal model is straightforward and has been well-documented in the literature [6].

However, without prior knowledge of the expected signal phase to allow application of a matched filter, time of arrival estimates are commonly computed from the received signal envelope

$$y_n = |x_n| = |a_n e^{j\phi_n} + w_n|, \quad n = 1 \dots N. \quad (2)$$

The envelope signal consists of samples with Rician density [7]

$$f(y_n) = \frac{2y_n}{\sigma^2} \exp\left\{-\frac{(a_n^2 + y_n^2)}{\sigma^2}\right\} \mathbf{I}_0\left(\frac{2y_n a_n}{\sigma^2}\right) u(y_n) \quad (3)$$

where $\mathbf{I}_0(\cdot)$ is the zeroth-order modified Bessel function of the first kind and $u(\cdot)$ is the unit step function. Continuing under the assumption of independent time samples, the joint

distribution over the complete signal $\underline{y} = \{y_1, y_2, \dots, y_N\}$ is

$$f(\underline{y}) = \prod_{n=1}^N f(y_n). \quad (4)$$

Information is lost in the envelope detection process, thus implying a loss in parameter estimation accuracy. Application of a Gaussian CRLB to an envelope signal may therefore fail to provide a tight bound under some operational conditions. Analyzing the lower bound on time of arrival estimates for a Rician distribution is more complex than for a Gaussian model, but as the next section shows, simple manipulations lead to an expression that may be efficiently evaluated.

III. CRAMÉR-RAO LOWER BOUND

The Cramér-Rao bound, which lower bounds the covariance of unbiased parameter estimates, is computed as the inverse of Fisher's information matrix

$$F_{ij}(\Theta) = E \left\{ \frac{\partial \log f(\underline{y}; \Theta)}{\partial \theta_i} \frac{\partial \log f(\underline{y}; \Theta)}{\partial \theta_j} \right\}, \quad (5)$$

such that

$$C(\hat{\Theta}) \geq F(\Theta)^{-1} \quad (6)$$

where $C(\hat{\Theta})$ is the covariance of unbiased estimates of the parameter set $\Theta = \{\theta_1, \dots, \theta_M\}$. Above, θ_i represents the i th parameter of the envelope signal a_n , and the CRLB on estimates of θ_i is defined as the $F_{ii}(\Theta)^{-1}$ element of the CRLB matrix. As the simulation results in Section IV will show, even in cases where estimates are not necessarily unbiased the CRLB is still informative.

While the CRLB's popularity is largely based on its ease of computation, populating Fisher's information matrix can still be challenging for statistical models that do not allow the expectation in (5) to be computed analytically. The Rician model (4) presents such a situation. In the following, two methods for computing the CRLB on Rician model parameters are presented. The first approach seeks to exactly populate Fisher's information matrix by computing the expectation in (5) through numerical integration. Some simple analytical steps are taken first to decompose (5) into a series of one-dimensional integrals that permit efficient and stable numerical computation. The second approach makes approximations to the envelope signal (2) to reach a model composed of higher-order Gaussian random variables. This allows the signal covariance to be computed analytically for use in Fisher's information matrix for Gaussian models, which approximates the Rician model at higher SNRs. The use of higher-order Gaussian moments in the covariance calculation will yield an approximated bound that is consistent with the numerically-computed Rician bound.

A. Numerical Solution

To numerically compute (5), we begin by calculating the derivative of the log-likelihood function with respect to each of

the model parameters, including time of arrival for our chosen application,

$$\begin{aligned} \frac{\partial \log f(\underline{y}; \Theta)}{\partial \theta_i} &= \frac{\partial}{\partial \theta_i} \sum_{n=1}^N \left[\log \frac{2y_n}{\sigma^2} - \frac{a_n^2 + y_n^2}{\sigma^2} \right. \\ &\quad \left. + \log I_0 \left(\frac{2y_n a_n}{\sigma^2} \right) \right] \\ &= \sum_{n=1}^N \left[I_0 \left(\frac{2y_n a_n}{\sigma^2} \right)^{-1} B_n - \frac{2a_n}{\sigma^2} \right] \frac{\partial a_n}{\partial \theta_i} \end{aligned} \quad (7)$$

where

$$B_n = \frac{\partial}{\partial a_n} I_0 \left(\frac{2y_n a_n}{\sigma^2} \right) = \frac{2y_n}{\sigma^2} I_1 \left(\frac{2y_n a_n}{\sigma^2} \right). \quad (8)$$

The exact form of these derivatives is specific to one's pulse shape model and constituent parameters. Inserting (7) into (5) gives

$$\begin{aligned} F_{ij}(\Theta) &= E \left\{ \sum_{n=1}^N \left[I_0 \left(\frac{2y_n a_n}{\sigma^2} \right)^{-1} B_n - \frac{2a_n}{\sigma^2} \right] \frac{\partial a_n}{\partial \theta_i} \right. \\ &\quad \left. \times \sum_{m=1}^N \left[I_0 \left(\frac{2y_m a_m}{\sigma^2} \right)^{-1} B_m - \frac{2a_m}{\sigma^2} \right] \frac{\partial a_m}{\partial \theta_j} \right\}. \end{aligned} \quad (9)$$

Evaluation of the above initially seems to imply the computation of a double integral – expectations over y_n and y_m that include the first order modified Bessel functions contained in B_n and B_m – for every sample in the signal envelope. As shown in the following, simple manipulations will reduce the calculation of (9) to a number of well-behaved single integrals.

Expanding (9) to yield

$$F_{ij}(\Theta) = \sum_{n=1}^N \sum_{m=1}^N \frac{\partial a_n}{\partial \theta_i} \frac{\partial a_m}{\partial \theta_j} K_{n,m} = \frac{\partial \underline{a}^T}{\partial \theta_i} K \frac{\partial \underline{a}}{\partial \theta_j}, \quad (10)$$

where

$$\begin{aligned} K_{n,m} &= E \left\{ I_0 \left(\frac{2y_n a_n}{\sigma^2} \right)^{-1} I_0 \left(\frac{2y_m a_m}{\sigma^2} \right)^{-1} B_m B_n \right\} \\ &\quad - \frac{2a_n}{\sigma^2} E \left\{ I_0 \left(\frac{2y_m a_m}{\sigma^2} \right)^{-1} B_m \right\} \\ &\quad - \frac{2a_m}{\sigma^2} E \left\{ I_0 \left(\frac{2y_n a_n}{\sigma^2} \right)^{-1} B_n \right\} + \frac{4a_n a_m}{\sigma^4} \end{aligned} \quad (11)$$

and

$$\frac{\partial \underline{a}}{\partial \theta_i} = \left[\frac{\partial a_1}{\partial \theta_i} \dots \frac{\partial a_N}{\partial \theta_i} \right]^T, \quad (12)$$

allows us to treat each term in (11) separately. The second and third expectations require computing single integrals of the form

$$\begin{aligned} &E \left\{ I_0 \left(\frac{2y_n a_n}{\sigma^2} \right)^{-1} B_n \right\} \\ &= \int_0^\infty \frac{4\tau^2}{\sigma^4} \exp \left\{ -\frac{a_n^2 + \tau^2}{\sigma^2} \right\} I_1 \left(\frac{2\tau a_n}{\sigma^2} \right) d\tau. \end{aligned} \quad (13)$$

While analytically intractable, the integrand is sufficiently smooth to allow a numerical integral to work efficiently and reliably.

The first expectation in (11) must be evaluated under two different cases dependent on the equality of n and m . For the case of $n \neq m$, the independence assumption allows the expectation to be separated into the product of two expectations

$$\begin{aligned} & E \left\{ I_0 \left(\frac{2y_n a_n}{\sigma^2} \right)^{-1} I_0 \left(\frac{2y_m a_m}{\sigma^2} \right)^{-1} B_m B_n \right\} \\ &= E \left\{ I_0 \left(\frac{2y_n a_n}{\sigma^2} \right)^{-1} B_n \right\} E \left\{ I_0 \left(\frac{2y_m a_m}{\sigma^2} \right)^{-1} B_m \right\}, \end{aligned} \quad (14)$$

which can be calculated separately via (13). When $n = m$, only a single integral is required

$$\begin{aligned} & E \left\{ I_0 \left(\frac{2y_n a_n}{\sigma^2} \right)^{-2} B_n^2 \right\} \\ &= \int_0^\infty \left[\frac{8\tau^3}{\sigma^6} \exp \left\{ -\frac{a_n^2 + \tau^2}{\sigma^2} \right\} \right. \\ &\quad \left. \times I_0 \left(\frac{2\tau a_n}{\sigma^2} \right)^{-1} I_1 \left(\frac{2\tau a_n}{\sigma^2} \right)^2 d\tau \right]. \end{aligned} \quad (15)$$

This result is similarly well-behaved for efficient numerical integration.

Combining (13), (14), and (15) allows the matrix K in (11) to be pre-computed for every sample in $n = 1 \dots N$. Then, combining these results with the derivative of the pulse envelope model a_n with respect to each parameter permits the Fisher's information matrix to be efficiently populated via (10). By comparison, brute force calculation of (9) would require N^2 numerical double integrals, while the proposed approach exploits redundancies to require only $2N$ numerical single integrals.

B. Approximate Solution

In the case of a deterministic signal vector corrupted by circular white Gaussian noise with variance σ^2 , the Fisher's information matrix for the signal parameters is well-known to be in the form expressed in (10) with $K = I2\sigma^{-2}$ [6]. As mentioned in the introduction, the Gaussian CRLB has frequently been used in the past to lower bound the variance of estimates obtained from the signal envelope. This approximation is effective at high SNR (*e.g.*, ≥ 20 dB), but does not provide a tight bound at lower signal-to-noise ratios. To obtain a tighter approximation to the Rician CRLB, we will approximate Fisher's information matrix in (10) as

$$F_{ij}(\Theta) \approx \frac{\partial a^T}{\partial \theta_i} P^{-1} \frac{\partial a}{\partial \theta_j} \quad (16)$$

where $K^{-1} \approx P_{t,s} = \delta_{t,s} k(a_t, \sigma^2)$ approximates the variance of the measured envelope as a function of the noise power and the amplitude of the uncorrupted signal envelope. An approximation of this form will give the ease of computation of

a Gaussian bound while also encapsulating the multiplicative nature of a Rician model.

To arrive at an expression for $k(a_n, \sigma^2)$, we begin by applying a first-order Taylor approximation – assuming $w_n/a_n \ll 1$ – to the envelope calculation in (2) to yield

$$\begin{aligned} y_n &= \sqrt{a_n^2 + 2a_n \Re\{w_n\} + |w_n|^2} \\ &\approx a_n + \Re\{w_n\} + \frac{\Im\{w_n\}^2}{2a_n}, \quad n = 1 \dots N, \end{aligned} \quad (17)$$

where $\Re\{w_n\}$ and $\Im\{w_n\}$ indicate the real and imaginary parts of w_n , respectively. The variance of this expression, computed based on the Gaussian moments of w_n , is then

$$k(a_n, \sigma^2) = \frac{\sigma^2}{2} + \frac{\sigma^4}{8a_n^2}, \quad (18)$$

such that $K \approx P^{-1} \rightarrow I2\sigma^{-2}$ as SNR becomes large, thus converging to the commonly used Gaussian approximation.

IV. SIMULATION RESULTS

While the above described analysis is generally applicable to any pulse shape and parameterization, two simple models were selected for illustrative examples. The rectangular envelope model used to describe a_n in (1) is defined as a piecewise continuous function

$$a_n = \begin{cases} \frac{b}{2} \left[1 + \sin \left(\frac{\pi}{t_r} [nT_s - t_0] \right) \right], & \left[t_0 - \frac{t_r}{2}, t_0 + \frac{t_r}{2} \right) \\ b, & \left[t_0 + \frac{t_r}{2}, t_1 - \frac{t_f}{2} \right) \\ \frac{b}{2} \left[1 - \sin \left(\frac{\pi}{t_f} [nT_s - t_1] \right) \right], & \left[t_1 - \frac{t_f}{2}, t_1 + \frac{t_f}{2} \right) \\ 0, & \text{Otherwise,} \end{cases} \quad (19)$$

where b is the amplitude, t_r is the rise time, and t_f is the fall time. The sampling interval is T_s , such that the discrete sample times are nT_s for $n = 1 \dots N$. The times of arrival and departure are t_0 and t_1 , respectively, thus defining the pulse width as $\tau = t_1 - t_0$. Thus, the unknown parameter set is defined as $\Theta = \{b, t_0, t_1, t_r, t_f\}$ such that the CRLB on the variance of time of arrival estimates will be the C_{22} element of the CRLB matrix. The cosine envelope model is the second piecewise continuous function used and is defined by

$$a_n = \begin{cases} \frac{b}{2} \left[1 + \cos \left(\frac{\pi}{\tau} nT_s \right) \right], & [-2\tau, 2\tau] \\ 0, & \text{Otherwise,} \end{cases} \quad (20)$$

where in this case, $\tau = 2t_0$ to take advantage of symmetry. The unknown parameter set for the cosine envelope is defined as $\Theta = \{b, t_0\}$. Figure 1 shows the pulse envelopes defined by (19) and (20). The CRLB was computed for various signal-to-noise ratios for both the Gaussian case that is documented in [6] and the Rician case derived in Section III. Using the piecewise envelope functions, the derivatives with respect to each of the parameters can be computed analytically and applied to (10) and the derivation in [6]. Using the envelope parameters for the rectangular and cosine pulses given in Figure 1, the Gaussian and Rician CRLB on time of arrival estimates are computed, as well as the approximate bound defined by the inverse of (16). To provide a verification

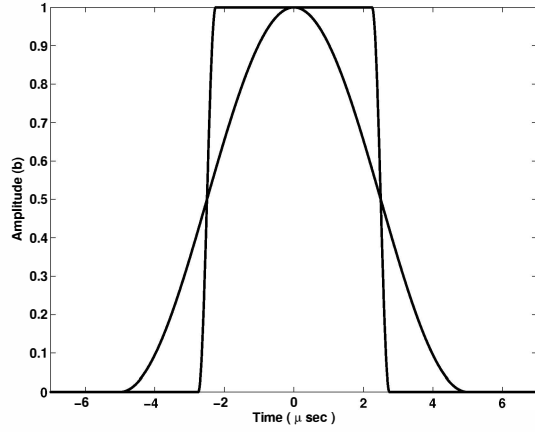


Fig. 1. Rectangular and Cosine Pulse Envelope for $F_s = 80\text{MHz}$, $\tau = 5\mu\text{sec}$ and $t_r = t_f = 500\text{nsec}$ (for rectangular pulse)

of the Rician CRLB results, a 10,000-iteration Monte Carlo simulation was performed using maximum likelihood, which is known to asymptotically achieve the CRLB, to estimate the pulse envelope parameters. A 10,000-iteration Monte Carlo simulation was also performed using least squares to give an upper bound for reference. For each maximum likelihood and least squares iteration, the estimator was seeded with the true parameter values, and then allowed to converge to the parameter set that maximizes (4). The maximum likelihood and least squares simulations were completed only for the rectangular pulse.

For both maximum likelihood and least squares, the time of arrival was estimated, and the root mean squared errors (RMSE) of their respective estimates were calculated. Figure 2 and 3 show the Gaussian CRLB, numerically-computed Rician CRLB, approximated Rician CRLB for the rectangular and cosine pulse, respectively. Figure 2 also displays the maximum likelihood RMSE and least squares RMSE for the rectangular envelope. As the SNR increases, the Rician density function behaves more like a Gaussian, and the respective bounds converge as seen in both figures, with the numerically-computed Rician CRLB consistently providing a tighter bound on algorithm performance than the Gaussian CRLB. The maximum likelihood RMSE curve and approximated Rician CRLB are consistent with the numerically-computed Rician CRLB in Figure 2. We note that the maximum-likelihood and least squares estimates are not unbiased, yet the CRLB curves still provide useful bounds on performance.

V. CONCLUSION

The Cramér-Rao Lower Bound was developed for parameter estimates from an envelope detected pulse. Bounds were derived for the Rician signal model using both a numerical method and a higher-order Gaussian approximation. The Gaussian and Rician CRLBs were compared to simulated time of arrival estimation performance to illustrate that the Rician model provides a tighter bound. Future work will include further envelope models with their corresponding parameter

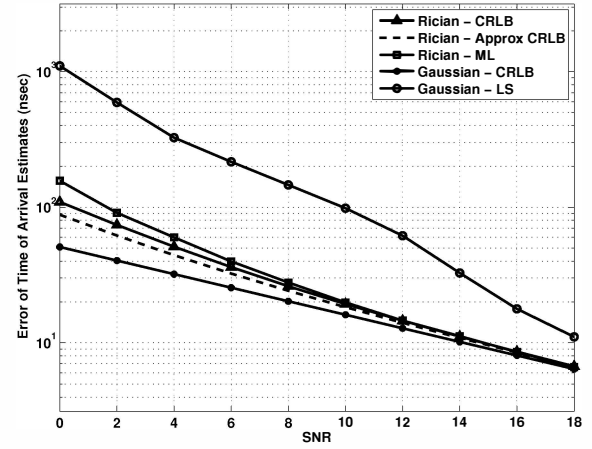


Fig. 2. Rician and Gaussian CRLB for time of arrival for the rectangular envelope model.

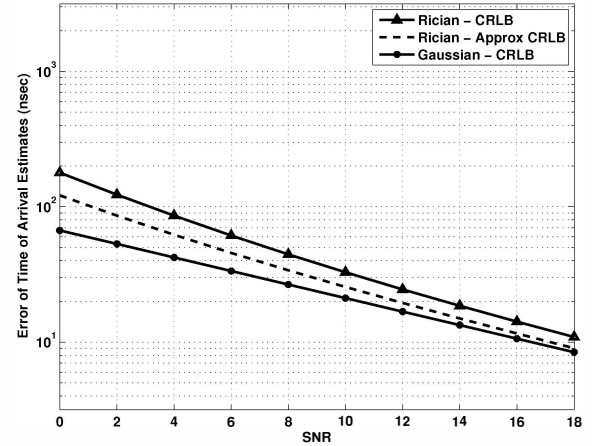


Fig. 3. Rician and Gaussian CRLB for time of arrival for the cosine envelope model

sets.

REFERENCES

- [1] David L. Adamy, *EW 101: A First Course in Electronic Warfare*. Norwood, Massachusetts: Artech House, 2001.
- [2] T. W. Fields, D. L. Sharpin, and J. B. Tsui, "Digital channelized IFM receiver," in *Telesystems Conference, 1994. Conference Proceedings., 1994 IEEE National*, San Diego, CA, May 1994, pp. 87–90.
- [3] D. R. Zahiriak, D. L. Sharpin, and T. W. Fields, "A hardware-efficient, multirate, digital channelized receiver architecture," *IEEE Transactions on Aerospace and Electronic Systems*, vol. 34, no. 1, pp. 137–152, Jan. 1998.
- [4] J. B. yen Tsui, *Digital Techniques for Wideband Receivers*. Raleigh, North Carolina: SciTech Publishing, 2004.
- [5] H. Cramér, *Mathematical Methods of Statistics*. Princeton University Press, 1946.
- [6] H. Ge and D.W. Tufts, "Cramér-Rao Lower Bounds on Estimating the Parameters of a Filtered Burst of Sinusoid," *IEEE Trans. Aerospace and Electronic Systems*, vol. 33, no. 2, pp. 421–431, April 1997.
- [7] H. Stark and J.W. Woods, *Probability, Random Processes, and Estimation Theory for Engineers*. Upper Saddle River, New Jersey: Prentice Hall, 1994.